Volume 2022, 20 pages | Article ID : IJPGE-2205292112788

International Journal of Petroleum and Geoscience Engineering

Journal homepage: www.htpub.org/ijpge/

ISSN: 2289-4713

Comparison and performance Analysis of Models for Predicting Multiphase flow Behaviours in Wellbores

Chibuzo Cosmas Nwanwe[a,b,*], Ugochukwu Ilozurike Duru[b]

[a]*Department of Minerals and Petroleum Resources Engineering Technology, Federal Polytechnic Nekede, Owerri, P.M.B. 1036, Owerri, Imo State, Nigeria*
[b]*Department of Petroleum Engineering, Federal University of Technology, Owerri, P.M.B. 1526, Owerri, Imo State, Nigeria*

Article

Article history
Received: 18 March 2022
Received in revised form: 22 April 2022
Accepted: 30 May 2022

Keywords:
Empirical correlations, mechanistic models, graphical error analysis, multiphase flow, statistical error analysis, relative error trend analysis

Abstract

Accurate predictions of flow pattern, liquid holdup, and pressure drop are essential factors for oil and gas wells analysis and production optimization. In the literature, there are several empirical correlations and mechanistic models for predicting pressure loss during multiphase flow in wellbores. This study presents a comparative and performance analysis of three empirical correlations and three mechanistic models. Open source real field well datasets were utilized to estimate the pressure drop using MATLAB scripts created for each of the investigated correlations and models. The performance of the investigated empirical correlations and mechanistic models is evaluated using statistical error analysis, graphical error analysis, and relative error trend analysis. The empirical correlations demonstrated the best estimation of the pressure drop according to the investigation results because of the large-scale data used in establishing the correlations and the modifications made. The mechanistic models demonstrated the worst performance prediction according to the investigation results because of severe under-prediction of the pressure drop by the mechanistic slug flow and churn flow models. A solution procedure is proposed in this study that would eliminate the issue of non-convergent solutions. More study is needed to modify and improve the mechanistic slug flow and churn flow models.

1. Introduction

Multiphase flow is the simultaneous existence of dynamic flow in several phases [1-3] and is usually encountered in the petroleum, nuclear, geothermal, and chemical industries [4-6]. The focus of this present study is the petroleum industry in which multiphase flow is encountered in petroleum drilling, production, transportation, and processing systems [5, 6]. In the first place, gas, oil, and water from onshore or offshore fields are produced through vertical, horizontal, or deviated wells and then transported through pipelines in hilly-terrains to processing facilities [7]. Secondly, it is customary to inject water, gas, or steam through vertical, horizontal, or deviated wells into the reservoir to improve

*Corresponding author at: Department of Minerals and Petroleum Resources Engineering Technology, Federal Polytechnic Nekede, Owerri, P.M.B. 1036, Owerri, Imo State, Nigeria
Email address: nwanwe.chibuzo@fpno.edu.ng

oil and gas production [7]. These two examples clearly show that multiphase flow in pipes of all inclination angles and direction of flow occurs often in the petroleum industry [8]. Multiphase flow occurrence in the petroleum industry presents the challenge of understanding, analyzing, and designing multiphase flow systems [9]. It is particularly economical to transport the produced fluids in long distant pipelines as two-phase mixtures as opposed to separating the mixture and transporting the individual phases separately [10]. This economic gain has further enhanced the significance of multiphase flow to the petroleum industry [10] and made petroleum companies invest heavily in multiphase flow modeling studies [11].

Multiphase flow in pipes is a more complicated phenomenon than single-phase flow because of the presence of different and difficult to identify flow patterns during multiphase flow [12]. This complex nature has over the years made modeling of multiphase flow challenging to researchers and field engineers [13, 14]. The identification and assessment of flow patterns are critical because liquid holdup and pressure drop [1] are heavily reliant on flow patterns in the design of production system equipment. As a result, reliable multiphase flow system design necessitates prior knowledge of the flow pattern [15]. Accurate prediction of flow pattern, liquid holdup, and pressure drop are essential ingredients for production optimization and analysis of oil and gas wells [13] as well a the construction and operation of multiphase flow pipelines [16]. Gas density, liquid density, solid density, gas superficial velocity, liquid superficial velocity, solid superficial velocity, pipe internal diameter, and inclination angle all have an impact on flow pattern, liquid holdup, and pressure drop [1, 17].

In the literature, there are several approaches for predicting multiphase bottom-hole flowing pressure in pipes. Empirical correlations, mechanistic models [18], and, most recently, machine learning models [19] are all examples of these methodologies.

The empirical correlations can further be classified as category A correlations [20-22], category B correlations [23, 24], and category C correlations [25-27] for no-slip and no-flow pattern consideration, slip and no-flow pattern consideration, and slip and flow pattern consideration respectively. These empirical correlations were developed by using experimental data to establish mathematical equations [9]. This use of experimental data has limited the applicability of the empirical correlations to the range of experimental data used in their development. Graphical correlations make empirical correlations difficult to code in a computer program.

Mechanistic models can also be classified as pipeline, wellbore, and unified mechanistic models for horizontal, vertical to slightly inclined and all inclination angles flow conditions respectively [28]. These models were formulated from physical laws and closed with closure empirical correlations. The applicability of mechanistic models is limited to the range of experimental data used in the development of the closure empirical correlations. These mechanistic models can be coded easily in a computer program because they don't contain any graphical correlations.

Artificial neural networks, Random forests, and K-Nearest Neighbors models are examples of machine learning models [29-32] that have been employed in the literature to estimate flowing bottom-hole pressure. These models lack a piece-wise calculation procedure and are limited by the total tubing length [31].

The objective is to analyze the performance of models used to predict multiphase flowing bottom-hole pressure (FBHP) in wellbores. This was achieved by predicting the multiphase FBHP with existing models and evaluating their accuracy with measured well data obtained from open source. Only empirical correlations and mechanistic models are considered in this evaluation.

2. Models for Predicting Multiphase Flow Behavior in Pipes

2.1. Empirical Correlations

Empirical correlations developed over the years for predicting multiphase flow behavior in pipes could be classified into three as category A, B, and C correlations [4].

2.1.1. Category A Correlations

Most of the earliest oil and gas wells were produced at high turbulent flow rates high enough for the gas and liquid to exist as a homogeneous mixture with the gas flowing at the same velocity as the liquid [33]. This observation of no slippage led to the development of Category A correlations, also known as homogeneous flow models, that treat multiphase flow as a perfectly homogeneous mixture flowing with no-slip between the phases. That is, category A correlations are based on no-slip assumptions and ignore flow patterns. The correlations developed by Fancher & Brown (1963), Poettmann & Carpenter (1952), and Baxendell & Thomas (1961) are only a few examples [20-22]. As one of the analyzed correlations in this study, the Poettmann & Carpenter (1952) correlation is briefly discussed.

The Poettmann & Carpenter (1952) correlation as shown in Equation (1) was developed with the aid of real field data measured from 49 gas lift and flowing wells. Poettmann & Carpenter's (1952) correlation predicts the pressure drop by using estimated values of the two-phase friction factor, f_{2F} and average no-slip mixture density, $\bar{\rho}_{mn}$. The two-phase friction factor, f_{2F} in Equation (1) was traditionally determined from correlations presented by Poettmann & Carpenter (1952) but recently from correlations developed by Guo & Ghalambor (2002) [22, 34].

$$\Delta p = \left(\bar{\rho}_{mn} + \frac{f_{2F} v_m^2 \bar{\rho}_{mn}}{2 g_c d}\right) \frac{\Delta h}{144} \tag{1}$$

Baxendell & Thomas (1961) and Fancher & Brown (1963) extended the applicability of the Poettmann & Carpenter (1952) friction factor correlation to higher rates and larger pipe sizes. That is; Baxendell & Thomas (1961), Fancher & Brown (1963), and Poettmann & Carpenter (1952) correlations differ only in the friction factor correlation.

2.1.2. Category B Correlations

It was observed that Category A correlations (homogeneous-flow models) were no longer accurate following the decline in the productivity of earlier wells [33]. This is because at lower rates, the gas and liquid no longer flowed at the same velocity, but rather the gas flowed at a velocity higher than the liquid. This observation of slippage leads to the development of Category B correlations which assume slip flow conditions but ignore flow patterns. Correlations developed by Asheim (1986) and Hagedorn & Brown (1965) are two examples. The original Hagedorn & Brown (1965) correlation is briefly reviewed because the modified Hagedorn & Brown (1965) correlation is one of the analyzed correlations.

Hagedorn & Brown (1965) measured pressure gradients during two-phase flow in 1 inch, 1.25 inch, and1.5-inch tubings at various liquid viscosities, liquid flow rates, and gas-liquid ratios using a 1500 ft vertical experimental well. The authors did not measure liquid holdup or flow patterns during the study. Rather the liquid holdup was calculated to agree with the measured pressure gradient after accounting for the acceleration and friction pressure gradients. The original Hagedorn & Brown (1965) correlation for pressure drop computations in vertical tubing in field units, with acceleration term neglected, is as given in Equation (2).

$$\Delta p = \left(\rho_{ms} + \frac{f_{2F} v_m^2 \rho_{mn}^2}{2 g_c d \rho_{ms}}\right) \frac{\Delta h}{144} \tag{2}$$

Where: ρ_{ms} is the slip mixture density, ρ_{mn} is the no-slip mixture density, v_m is the mixture velocity, f_{2F} is the two-phase friction factor, Δh is the length of tubing segment length and d is the diameter of the tubing segment.

In predicting liquid holdup, the original Hagedorn & Brown (1965) correlation uses three correlations based on Ros (1961) four dimensionless groups [24, 35]. The Hagedorn & Brown (1965) correlation is a Category B correlation because it assumes slip flow conditions but ignores flow patterns.

2.1.3. Category C Correlations

Although Category B correlations considered slip between the phases, they still treated multiphase fluid flow as a homogeneous mixture which is unrealistic. It's worth noting that a multiphase fluid isn't a homogeneous mixture; rather, the interface between gas and liquid exists in various geometrical shapes known as flow patterns [33]. These observations of slippage and flow patterns during multiphase flow result in the establishment of Category C correlations that are reliant on both slip and flow patterns. Beggs & Brill (1973), Duns Jr. & Ros (1963), Orkiszewski (1967), and modified Hagedorn & Brown (1965) correlations are just a few examples [24-27]. As one of the analyzed correlations, the modified Hagedorn & Brown (1965) correlation is briefly discussed. In addition, the original Beggs & Brill (1973) correlation is briefly reviewed because the modified Beggs & Brill (1973) correlation is one of the analyzed correlations.

It was found in certain situations, that the liquid holdup, H_L predicted by the original Hagedorn & Brown (1965) correlation was less than the no-slip liquid holdup, λ_L for vertical upward flows [36]. This was not physically possible because according to the definition, H_L must be greater than λ_L. This led to the modification of the original Hagedorn & Brown (1965) correlation. The first modification was done by setting H_L equal to λ_L if predicted H_L is less than λ_L. The second modification was achieved by using the Griffith & Wallis (1961) correlation as given by Equation (4) in computing the liquid holdup if bubble flow regime is predicted and the original Hagedorn & Brown (1965) correlation as given by Equation (2) if bubble flow regime is not predicted [24, 37]. The bubble flow regime is predicted if the input gas fraction λ_g is less than the input gas fraction at the bubble-slug transition, L_B as given by Equation (3).

$$L_B = 1.071 - 0.2218(v_m^2/d) \qquad L_B \geq 0.13 \text{ is valid.} \tag{3}$$

where v_m is the velocity of the mixture and d is the internal diameter of the tubing.

$$\Delta p = \left(\rho_{ms} + \frac{f_{LF} v_L^2 \rho_L^2}{2 g_c d \rho_L H_L^2}\right)\frac{\Delta h}{144} \tag{4}$$

It became evident that the empirical correlations developed for vertical wells failed when applied to directional wells. This motivated researchers [25, 38] to develop correlations applicable to directional wells and hilly-terrain pipelines. Beggs & Brill (1973) conducted 584 two-phase flow experiments in a test facility consisting of 90 ft long acrylic pipe with diameters of 1 inch and 1.5 inches with a multiphase fluid of air and water. For each pipe size, the test was carried out by placing the pipe horizontally and then adjusting the liquid and gas rates to examine all flow patterns when the pipe was horizontal. Then, while altering the liquid and gas rates for each inclination angle, the inclination angles were altered in the range of $+90°$ to $-90°$ to observe the influence of inclination angle on liquid holdup and pressure gradient. The liquid holdup and pressure gradient at angles of $0°$, $\pm 5°$, $\pm 10°$, $\pm 15°$, $\pm 20°$, $\pm 35°$, $\pm 55°$, $\pm 75°$ and $\pm 90°$ from the horizontal were measured [18]. The original flow pattern map presented by Beggs & Brill (1973) consists of segregated, intermittent, and distributed flow regimes and has been modified with the inclusion of the transition flow regime between the segregated and intermittent flow regimes [39]. The location of the no-slip liquid holdup, λ_L and the Froude number, N_{Fr} on modified Beggs & Brill (1973) flow pattern map gives the flow pattern that would exist if the pipe were horizontal. The

Beggs & Brill (1973) correlation for calculating the pressure traverse in inclined pipes, including the contribution of the dimensionless kinetic energy, E_k is as given in Equation (5).

$$\left(\frac{dp}{dL}\right)_t = \frac{\left(\frac{dp}{dL}\right)_{el} + \left(\frac{dp}{dL}\right)_f}{1 - E_k} \tag{5}$$

where

$$\left(\frac{dp}{dL}\right)_{el} = \frac{g\rho_{ms}\sin\theta}{g_c} \tag{6}$$

$$\left(\frac{dp}{dL}\right)_f = \frac{f_{2F}\rho_{nm}v_m^s}{2g_c d} \tag{7}$$

$$E_k = \frac{\rho_{ms}v_m v_{sg}}{g_c p} \tag{8}$$

The Beggs & Brill (1973) correlation is slip and flow pattern dependent and hence classified as a Category C correlation. According to Payne et al. (1979), the original Beggs & Brill (1973) correlation overpredicted liquid holdup in uphill and downhill flows and also underpredicted the two-phase friction factor [25, 40]. First, the authors recommended 0.924 and 0.685 as correction factors for the liquid holdup in uphill and downhill flows respectively. Second, they recommended the Moody diagram be used to determine the normalizing friction factor, f_n. The modified Beggs & Brill (1973) correlation considered in this study is the original Beggs & Brill (1973) correlation with the correction proposed by Payne et al. (1979).

2.2. Mechanistic Models

Comprehensive mechanistic models are developed to first predict flow patterns with the aid of a flow pattern prediction model. The hydrodynamic model that corresponds to the predicted flow pattern is then employed in liquid holdup and pressure drop computations [6]. Comprehensive mechanistic models developed over the years can be classified as pipeline, wellbore, and unified mechanistic models [28].

2.2.1. Pipeline Mechanistic Models

Pipeline mechanistic models can be used for horizontal to near horizontal ($-10° \leq \theta \leq +10°$) flow conditions [28]. Mechanistic models by Xiao et al. (1990) and Ouyang & Aziz (2002) are two examples [41, 42].

Xiao et al. (1990) extended on the previous work of Barnea et al. (1980) and Taitel & Dukler (1976) by developing the first comprehensive mechanistic model for gas-liquid flow in horizontal to near horizontal pipelines [15, 42, 43]. Their approach includes a flow pattern prediction model as well as distinct hydrodynamic models for the various flow patterns. The authors compared the performance of their model to that of the most prevalent two-phase flow pipeline correlations using a pipeline data bank. Their mechanistic model beat all pipeline correlations published before 1990, according to the findings. In their model, Xiao et al. (1990) ignored froth and elongated bubble flow patterns.

Ouyang & Aziz (2002) established a mechanistic model for predicting multiphase flow behavior in horizontal wells that accounts for wall outflow or inflow effects on flow pattern transitions, wall friction, and acceleration. Their approach includes a flow pattern prediction model as well as distinct hydrodynamic models for the various flow patterns, which include bubble, intermittent, stratified, and annular-mist flow patterns. No distinction was made between slug and elongated bubble flow patterns, instead, they were considered as part intermittent flow. Their model and some existing models were employed in the flow pattern and pressure drop predictions for the Stanford-Marathon horizontal wellbore experiments of 1995 to 1997 and the predicted results compared with experimentally measured data. Their model outperformed existing models in predicting flow patterns and pressure drops in horizontal wellbores [41].

2.2.2. Wellbore Mechanistic Models

Wellbore mechanistic models apply for vertical to sharply inclined ($60° \leq \theta \leq 90°$) flow conditions [28]. Several comprehensive mechanistic models have also been developed over the years for predicting gas-liquid flow behavior in vertical wells [4, 44, 45] as well as in sharply inclined or deviated wells [5, 6, 46]. These mechanistic models first predict the flow pattern existing in the well or pipe section and then employ the actual mechanisms of the predicted flow pattern in computing the holdup, and pressure gradient [18]. As one of the analyzed mechanistic models, the Hasan & Kabir (1988a) and Ansari et al. (1994) models are briefly discussed.

An approach similar to the Taitel et al. (1980) flow pattern transition was adopted by Hasan & Kabir (1988a) in developing a mechanistic model that could be used to predict flow pattern, void fraction, and pressure gradient in vertical wells. Their model prediction was shown to be in excellent agreement with laboratory data for all flow patterns except churn flow [46, 47].

A comprehensive mechanistic model was later formulated by Ansari et al. (1994) for predicting multiphase flow behavior in vertical wells. Their model consists of a flow pattern prediction model and a series of independent hydrodynamic models for liquid holdup and pressure drop prediction for all flow patterns except the churn flow. Because of the complexity of churn flow, the authors considered it as a subset of slug flow. The overall model performance of Ansari et al. (1994) model was found to be in good agreement with the oil well data bank. Six empirical correlations and the Hasan & Kabir (1988a) mechanistic model performed worse than the Ansari et al. (1994) model.

2.2.3. Unified Mechanistic Models

Unified mechanistic models can be used for horizontal ($0°$) to vertical upward flow ($+90°$) and for vertical downward flow ($-90°$) conditions [48]. The incorporation of the angle of inclination makes unified mechanistic models more practical than pipeline and wellbore mechanistic models [28]. Examples include mechanistic models developed by Gomez et al. (2000), Petalas & Aziz (2000), Zhang et al. (2003a), and Zhang & Sarica (2006) [7, 8, 28, 48]. As one of the analyzed mechanistic models, the Petalas & Aziz (2000) model is briefly discussed.

Petalas & Aziz (2000) presented a unified mechanistic model that could be applied to pipes of all geometries and fluid properties. The authors proposed new closure empirical correlations in annular-mist flow, stratified flow, and intermittent flow. Their model was found to be more robust than existing models after undergoing extensive testing against laboratory and field data.

2.3. Machine Learning Models

It is evident from experience that empirical correlations and mechanistic models have failed to provide a reliable and satisfactory prediction of pressure drop during multiphase flow in pipes [29]. This has motivated researchers to use machine learning models in predicting bottom-hole pressure in oil wells. Several machine learning (ML) models have been reported in the literature but the most widely used in the petroleum industry for predicting multiphase flow behavior in pipes is the Artificial Neural Network.

Jahanandish et al. (2011) used 413 Irian oil field data to develop an ANN model flowing bottom-hole pressure prediction. Their ANN model performed better than existing empirical correlations and mechanistic models [29].

Li et al. (2014) developed a procedure for computing bottom-hole pressure that couples empirical correlations and backpropagation ANN models. Their coupled procedure gave better predictions than the empirical correlations [31].

Sami & Ibrahim (2021) employed three ML techniques (artificial neural networks, random forests, and K-Nearest Neighbors) in developing ML models for predicting bottom-hole pressure in wellbores. The results of their study showed that ANN outperformed random forest and K-Nearest Neighbors [32].

Kanin et al. (2019) developed an ML model that uses three surrogate models nested within each other for predicting multiphase flow behavior in pipes, Their model performed better than the Mukherjee & Brill (1985) correlation and the combined Ansari et al. (1994) and Xiao et al. (1990) models [4, 30, 38, 42].

Abdul-Majeed et al. (2022) used 2525 experimental datasets to develop an ANN visible mathematical model for predicting slug liquid holdup (ANN-H_{LS}) in pipes of all angles of inclination [49]. A comparative study showed that the developed ANN-H_{LS} model outperformed 12 different slug liquid holdup correlations. Furthermore, the authors combined the developed ANN-H_{LS} model with the mechanistic slug flow models of Abdul-Majeed & Al-Mashat (2000) and Zhang et al. (2003a) [7, 50]. Statistical results showed that the combined ANN-H_{LS} with mechanistic slug flow model outperformed existing mechanistic slug flow models.

3. Evaluation Procedure

3.1. Data Collection

The gathering of data is the initial stage in comparing and contrasting various empirical correlations and mechanistic models. This evaluation research requires representative data. Ayoub (2004) gathered 386 well data sets from Middle Eastern fields and reduced them to 206 well data sets by removing unrepresentative data using existing empirical correlations and mechanistic models. As a result, the 206 well data sets used by Ayoub (2004) were used in this analysis since they are representative [19]. The data set consists of nine input production parameters and one output production parameter. The input production parameters include oil flow rate, water flow rate, gas flow rate, the internal diameter of the tubing, well perforation depth, oil API gravity, wellhead temperature, well bottom-hole temperature, and wellhead pressure [32]. The flowing bottom-hole pressure [32] is the output production data. Table 1 shows the statistical analysis of the oil field well dataset employed in this study.

Table 1. Statistical analysis of oil field well dataset employed in the comparative study

S/N	Production Parameters	Units	Min	Max	Average	STD
1.	Oil flow rate	stb/d	280.00	19618.00	6321.51	4835.16
2.	Water flow rate	stb/d	0.00	11000.00	2700.01	2793.08
3.	Gas flow rate	$Mscf/d$	33.60	13562.20	3416.07	3068.44
4.	Internal diameter of the tubing	$inch$	2.00	4.00	3.83	0.39
5.	well perforation depth	$feet$	4550.00	7100.00	6359.87	566.28
6.	Oil API gravity	$°API$	30.00	37.00	33.77	2.32
7.	Wellhead temperature	°F	76.00	160.00	117.73	30.79
8.	Well bottom-hole temperature	°F	157.00	215.00	203.64	16.96
9.	Wellhead pressure	$psia$	80.00	960.00	321.08	153.56
10.	Flowing bottom-hole pressure	$psia$	1227.00	3217.00	2489.03	302.17

3.2. Predictive Multiphase Flow Models Selected for Comparative Study

Based on the extensive literature review conducted in this study, three mechanistic models and three empirical correlations were selected for evaluation. The Poettmann & Carpenter (1952), modified Hagedorn & Brown (1965), and modified Beggs & Brill (1973) correlations were the empirical correlations used in the comparative analysis [22, 24, 25]. The Ansari et al. (1994), Hasan & Kabir

(1988a), and Petalas & Aziz (2000) models were the mechanistic models employed in the comparative analysis [4, 44, 48].

The second step in the evaluation process involved the use of MATLAB to code the three selected empirical correlations and three selected mechanistic models. Pressure transverse calculations for all considered empirical correlations and mechanistic models were performed against the direction of flow by first dividing the tubing into segments of equal length. The solution procedure presented in the previous work of Nwanwe et al. (2020) was adopted here [51]. The in-situ volumetric flow rates of the gas, oil and water phases required for computation of the gas, oil, and water superficial velocities were computed with the aid of Equations (9), (10), and (11) respectively. The pressure at the bottom of the tubing for each of the Ayoub (2004) 206 well data cases were then predicted using the MATLAB scripts for each of the specified empirical correlations and mechanistic models.

$$q_g(k) = \left[1000q_{gsc} - q_{osc}R_{so}(k) - q_{wsc}R_{sw}(k)\right]B_g(k) \tag{9}$$

$$q_o(k) = \frac{5.615q_{osc}B_o(k)}{86400} \tag{10}$$

$$q_w(k) = \frac{5.615q_{wsc}B_w(k)}{86400} \tag{11}$$

where: q_{gsc} is the gas production rate, q_{osc} is the oil production rate, q_{wsc} water production rate, $R_{so}(k)$ is the solution gas-oil ratio, $R_{sw}(k)$ is the solution gas-water ratio, $B_g(k)$ is the gas formation volume factor, $B_o(k)$ is the oil formation volume factor, $B_w(k)$ is the water formation volume factor, $q_g(k)$ is the gas in-situ volumetric flow rate, $q_o(k)$ is the oil in-situ volumetric flow rate, and $q_w(k)$ is the water in-situ volumetric flow rate.

The solution gas-water ratio and solution gas-oil ratio were computed as functions of temperature and pressure with the aid of the Ahmed (1989) and Standing (1981) correlations respectively [52, 53]. The gas, oil, and, water formation volume factors were also computed as functions of pressure and temperature with the aid of the gas formation volume factor equation, Standing (1981) correlation, and Gould's (1974) polynomial empirical relationship respectively [53, 54].

While evaluating the MATLAB programs of the specified empirical correlations and mechanistic models, the authors of this study noticed that some field well datasets produced non-convergent solutions (NCS). These NCS have also been reported in the literature [5, 6]. After more research, it was discovered that these NCS were caused by the gas in-situ rate, $q_g(k)$ as given by Equation (9) becoming negative at very high pressures. These negative $q_g(k)$ values are physically impossible but could be explained by the fact that at pressures greater than the bubble point pressure, the gas is completely dissolved in the oil, with no visible bubbles. This implies that the gas is not flowing at this point. Based on this explanation, we solved the problem of NCS by setting $q_g(k)$ equal to zero if the predicted $q_g(k)$ as defined by Equation (9) is negative. This solution procedure eliminated the problem of NCS.

The predicted pressure at the bottom of the tubing is then recorded in an excel spreadsheet for each of the 206 well data cases. Following that, Equations (12) and (13) are used to calculate the measured and predicted pressure drops, respectively.

$$\Delta p_{i_{meas}} = p_{bhi_{meas}} - p_{whi_{meas}} \tag{12}$$

$$\Delta p_{i_{pred}} = p_{bhi_{pred}} - p_{whi_{meas}} \tag{13}$$

where: $\Delta p_{i_{meas}}$ is the measured pressure drop, $\Delta p_{i_{pred}}$ is the predicted pressure drop, $p_{bhi_{meas}}$ is the measured bottom-hole pressure, $p_{bhi_{pred}}$ is the predicted bottom-hole pressure and $p_{whi_{meas}}$ is the measured wellhead pressure.

The accuracy of the selected empirical correlations and mechanistic models is checked using error analysis approaches in this work. These error analysis techniques include statistical error analysis [4] and graphical error analysis [19].

3.3. Statistical Error Analysis

Statistical error analysis is employed to check the accuracy of each of the selected empirical correlations and mechanistic models using the Ayoub (2004) 206 well cases. The statistical error analysis is based on the statistical parameters as originally defined by Ansari et al. (1994). These statistical parameters include absolute average percent error, average percent error, percent standard deviation, absolute average error, average error, standard deviation, and relative performance factor.

3.3.1. Average Percent Error

The average percent error, E_1, as given in Equation (14), is a measure of the difference between the measured and predicted pressure drops relative to the measured pressure drop [55] and represents the overall performance trend relative to the measured pressure drop [4-6]. A positive average percent error, E_1 shows that the pressure drop was over-predicted, whereas a negative average percent error shows that the pressure drop was underpredicted.

$$E_1 = \frac{1}{n}\left(\sum_{i=1}^{n} e_{ri}\right) \tag{14}$$

where: e_{ri} is the relative error of the ith data set and indicates how accurate is the predicted pressure drop relative to the measured pressure drop [55, 56] and is as given in Equation (15).

$$e_{ri} = \frac{\Delta p_{i_{pred}} - \Delta p_{i_{meas}}}{\Delta p_{i_{meas}}} \tag{15}$$

3.3.2. Absolute Average Percent Error

Absolute average percent error, E_2, as given in Equation (16), represents the average size of the errors [4]. E_2 does not allow the negative and positive relative errors to cancel out [5, 6] and this is why E_2 is considered a more meaningful statistical parameter than E_1 [55].

$$E_2 = \frac{1}{n}\left(\sum_{i=1}^{n} |e_{ri}|\right) \tag{16}$$

3.3.3. Percent Standard Deviation

Percent standard deviation, E_3, as given in Equation (17), indicates the degree of error dispersal around the average value [4].

$$E_3 = \sum_{i=1}^{n} \sqrt[2]{\frac{(e_{ri} - E_1)^2}{n-1}} \tag{17}$$

3.3.4. Average Error

The average error, E_4, as given in Equation (18), is the measure of the difference between the measured and predicted pressure drops independent of the measured pressure drop [55] and represents the overall performance trend independent of the measured pressure drop [4-6].

$$E_4 = \frac{1}{n}\left(\sum_{i=1}^{n} e_i\right) \tag{18}$$

where: e_i is the actual error of the ith data set and indicates how accurate is the predicted pressure drop independent of the measured pressure drop [55, 56] and is as given in Equation (19). A positive and negative average error indicates over-prediction and under-prediction of the pressure drop respectively.

$$e_i = \Delta p_{i_{pred}} - \Delta p_{i_{meas}} \tag{19}$$

3.3.5. Absolute Average Error

The absolute average error, E_5, as given in Equation (20), represents the magnitude of the difference between the measured and predicted pressure drops independent of the measured pressure drop [4] and does not allow the negative and positive actual errors to cancel out [55].

$$E_5 = \frac{1}{n}\left(\sum_{i=1}^{n} |e_i|\right) \tag{20}$$

3.3.6. Standard Deviation

Standard deviation, E_6, as given in Equation (21), indicates the degree of error dispersal independent of the measured pressure drop [4].

$$E_6 = \sum_{i=1}^{n} \sqrt[2]{\frac{(e_i - E_4)^2}{n-1}} \tag{21}$$

The statistical parameters defined by Equations (14), (16), and (17) are based on the errors relative to the measured pressure drop and are suited for evaluating small error values [57]. The statistical parameters defined by Equations (18), (20), and (21) on the other hand are based on actual errors and are better suited for evaluating large error values [57].

3.3.7. Relative Performance Factor

The relative performance factor, F_{rp} as defined by Equation (22), was recommended by Ansari et al. (1994) for making a comparison between the correlations and models with a minimum value of 0 for the best performance prediction and maximum value of 6 for the worst performance prediction. Relative performance factor, F_{rp} is the most important statistical error parameter because it incorporates the effects of all the statistical errors and deviations (E_1, E_2, E_3, E_4, E_5 and E_6) as defined in Equation (22).

$$F_{rp} = \frac{|E_1| - |E_{1_{min}}|}{|E_{1_{max}}| - |E_{1_{min}}|} + \frac{E_2 - E_{2_{min}}}{E_{2_{max}} - E_{2_{min}}} + \frac{E_3 - E_{3_{min}}}{E_{3_{max}} - E_{3_{min}}} + \frac{|E_4| - |E_{4_{min}}|}{|E_{1_{max}}| - |E_{4_{min}}|} + \frac{E_5 - E_{5_{min}}}{E_{5_{max}} - E_{5_{min}}} + \frac{E_6 - E_{6_{min}}}{E_{6_{max}} - E_6} \tag{22}$$

3.4. Graphical Error Analysis

Graphical error analysis was used in this work to visualize the accuracy of the selected correlations and models. Graphical error analysis employed includes cross-plots and residual analysis.

3.4.1. Cross-plot

Cross-plots were constructed by first plotting all the predicted pressure drop values of the selected empirical correlations and mechanistic models on the Y-axis against the measured pressure drop values on the X-axis. Next, a line of unit slope (45^o straight line), which represents a perfect correlation line, is drawn through the origin [58]. The closer the plotted points are to the unit slope line, the better is the correlation between the predicted and measured pressure drop [19]. Deviation lines of +20% and -20% are also plotted to visualize the over-prediction and under-prediction respectively of the different correlations and models. Cross-plots are important because it helps in the identification of the number of possible outliners [30].

3.4.2. Residual Analysis

Residual analysis is performed by plotting the actual error, e_i as defined by Equation (19) on the Y-axis and the oil field well dataset numbers on the X-axis. The plot will show the distribution of the actual error around the zero error line and as a result, it's a useful tool for detecting deficiencies [19] of the selected empirical correlations and mechanistic models. Residual deviation lines of +300 psi and -300 psi are also plotted for ease in visualizing the over-prediction and under-prediction respectively of the different correlations and models.

3.5. Relative Error Trend Analysis

We observed that the investigated mechanistic models underpredicted the pressure drop more than the empirical correlations. On further investigation of this observation, we found out that the considered mechanistic models underpredicted the pressure drop whenever slug flow is predicted for Ansari et al. (1994) and Petalas & Aziz (2000) models and churn flow for the Hasan & Kabir (1988a) model. A decision was made by the authors to perform a relative error trend analysis to visualize how the relative error varies as the percent of tubing with a slug or churn flow predicted by the investigated mechanistic models increases. To do this, the pressure transverse calculations were done by dividing the tubing into several tubing segments, N_{TS} of equal length. At the end of each prediction, the bottom-hole pressure and number of tubing segments with slug flow or churn flow predicted, N_{FL} are recorded on an excel spreadsheet. This is done for all 206 well data sets and each of the three investigated mechanistic models. The relative error for each data set is computed by applying Equations (12), (13) and (15) while the percent of tubing with a slug flow or churn flow predicted, P_{FL} is computed with Equation (23).

$$P_{FL} = 100 * \left(\frac{N_{FL}}{N_{TS}}\right) \tag{23}$$

The relative error trend analysis was performed by plotting the relative error on the Y-axis and the percent of tubing with slug or churn flow predicted by the investigated mechanistic models on the X-axis. A trend line is added to the plot. Upward and downward trend lines indicate over-prediction and under-prediction respectively of the pressure drop as the percent of tubing with a slug or churn flow predicted by the investigated mechanistic models increases.

4. Results

4.1. Statistical Error Analysis Results

Table 2 shows the results of the statistical error analysis for pressure drop prediction using selected empirical correlations and mechanistic models based on Ayoub's (2004) 206 well cases. The second row, columns 3 through 5 identifies the considered empirical correlations while the second row, columns 6 through 8 identifies the considered mechanistic models. The statistical error parameters E_1 through E_6 are given in rows 3 through 8. The relative performance factor, F_{rp} is reported on the ninth row. For each row, the values in brackets are the performance prediction position of each of the correlations and models for each of the considered statistical parameters. Positions (1) and (6) represent the best and worst performance predictions respectively.

Table 2. Results of statistical error analysis for all considered correlations and models based on the Ayoub (2004) 206 well cases.

		Empirical Correlations			Mechanistic Models		
Statistical Parameters	**Units**	**PC**	**HB**	**BB**	**AN**	**HK**	**PA**
E_1	%	-5.18 (2)	-1.46 (1)	-7.90 (3)	-22.66 (6)	-16.19 (5)	-13.92 (4)
E_2	%	14.17 (3)	8.08 (1)	8.87 (2)	23.38 (6)	19.43 (5)	15.01 (4)
E_3	%	191.65 (4)	115.87 (2)	85.67 (1)	229.05 (5)	243.67 (6)	145.65 (3)
E_4	psia	-119.99 (2)	-21.43 (1)	-169.48 (3)	-501.30 (6)	-362.17 (5)	-305.32 (4)
E_5	psia	310.34 (3)	171.01 (1)	188.28 (2)	511.99 (6)	423.28 (5)	325.04 (4)
E_6	psia	4192.94 (4)	2444.14 (2)	1760.84 (1)	5116.56 (5)	5359.15 (6)	3169.59 (3)
F_{rp}	-	2.53 (3)	0.38 (1)	0.71 (2)	5.84 (6)	4.88 (5)	2.67 (4)

4.2. Graphical Error Analysis Results

4.2.1. Cross-plot Results

Figure 1 shows the measured and predicted pressure drops cross-plots for the investigated empirical correlations and mechanistic models.

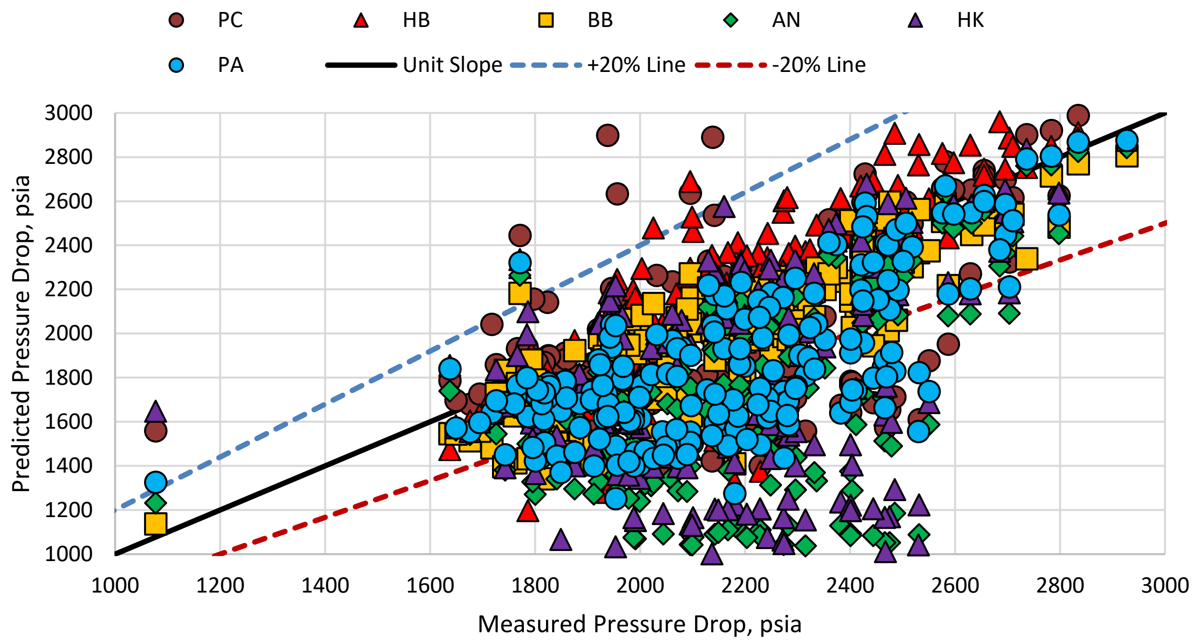

Figure 1. Pressure drop cross-plots for investigated empirical correlations and mechanistic models.

4.2.2. Residual Analysis Results

Figure 2 shows the residual plots for the investigated empirical correlations and mechanistic models.

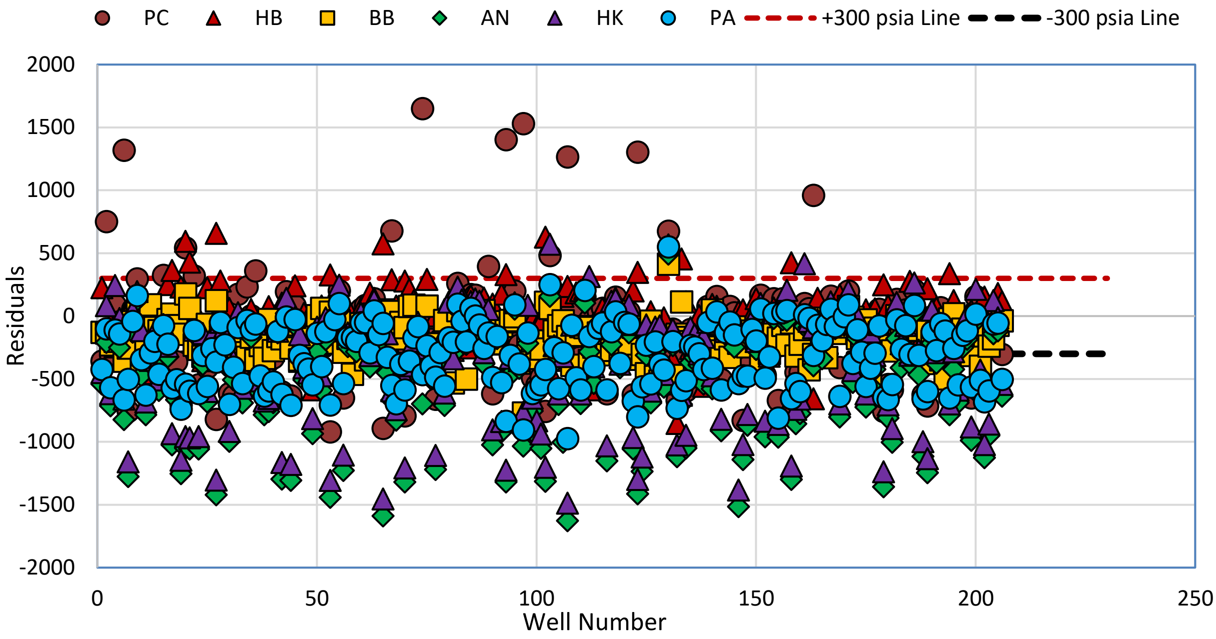

Figure 2. Residual plots for the investigated empirical correlations and mechanistic models

4.3. Trend Analysis Results

Figure 3 shows the trend analysis plots for all the investigated mechanistic models.

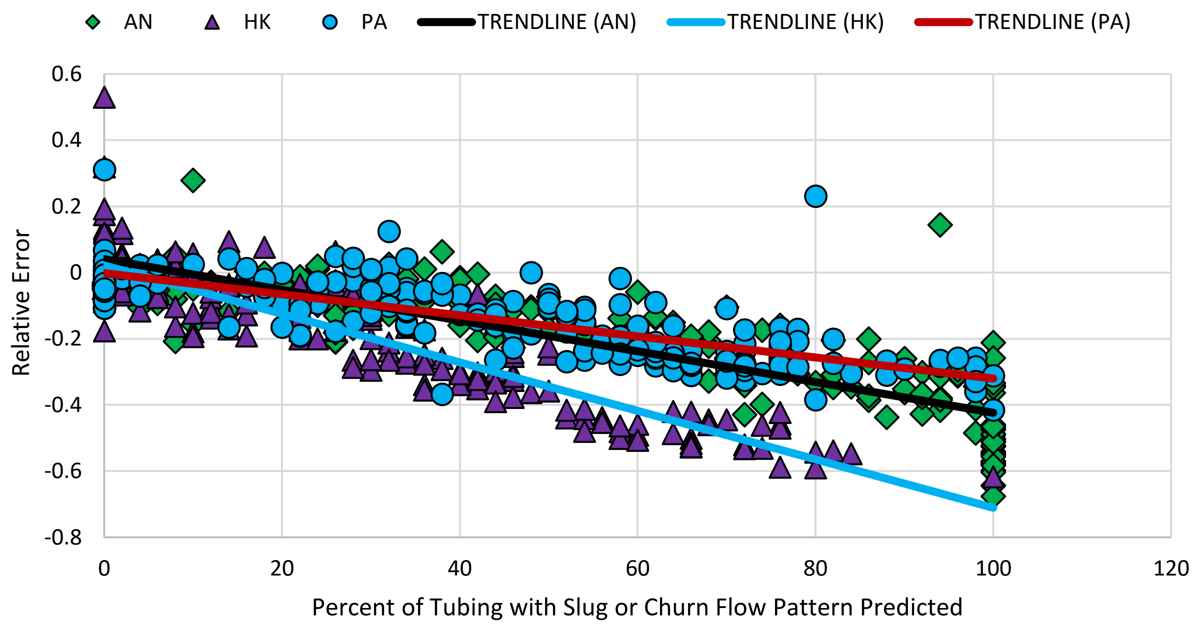

Figure 3. Trend analysis plots for investigated mechanistic models.

5. Discussion

5.1. Discussion on Statistical Error Analysis Results

A positive average percent error, E_1 indicates pressure drop overprediction, whereas a negative average percent error indicates pressure drop underprediction. In other words, the more negative is the value of E_1, the higher is the tendency for the correlation or model to underpredict the pressure drop and vice versa. As shown in Table 2, the most negative value of E_1 (-22.66%) was achieved by the Ansari et al. (1994) model, implying it underpredicts the pressure drop the most (worst performance). On the other hand, the least negative value of E_1 (-1.46%) was achieved by the modified Hagedorn & Brown (1965) correlation, implying it underpredicts the pressure drop the least (best performance). Based on E_1, the performance ranking of the investigated empirical correlations and mechanistic models decrease in the order of modified Hagedorn & Brown (1965) correlation, Poettmann & Carpenter (1952) correlation, modified Beggs & Brill (1973) correlation, Petalas & Aziz (2000) model, Hasan & Kabir (1988a) model and, Ansari et al. (1994) model. It's worth noting that the mechanistic models underpredicted the pressure drop more than the empirical correlations. On further investigation of this observation, we found out that the considered mechanistic models underpredicted the pressure drop whenever slug flow is predicted for Ansari et al. (1994) and Petalas & Aziz (2000) models and churn flow for the Hasan & Kabir (1988a) model.

The absolute average percent error, E_2 represents the average size of the errors [4]. Table 2 shows that the highest E_2 value (23.38%) was achieved by the Ansari et al. (1994) model, implying that it was the most incorrect (worst performance). On the other hand, the lowest value of E_2 (8.08%) was achieved by the modified Hagedorn & Brown (1965) correlation, implying that it was the most accurate (best performance). The performance ranking of the considered correlations and models decreased in the order of modified Hagedorn & Brown (1965) correlation, modified Beggs & Brill (1973) correlation, Poettmann & Carpenter (1952) correlation, Petalas & Aziz (2000) model, Hasan & Kabir (1988a) model, and Ansari et al. (1994) model. The performance ranking positions of the correlations and models concerning E_2 are the same as that for E_1 with a difference that modified Beggs & Brill (1973) correlation and Poettmann & Carpenter (1952) correlation are on the second and third performance ranking positions respectively. As in E_1, the empirical correlations performed better than the mechanistic models when E_2 is considered.

Percent standard deviation, E_3 indicates the degree of error dispersal around the average value [4]. As shown in Table 2, the Hasan & Kabir (1988a) model had the highest value of E_3 (243.67%), implying the greatest degree of error dispersal around the average value (worst performance). The modified Beggs & Brill (1973) correlation had the lowest value of E_3 (85.67%) which implies the lowest degree of error dispersal around the average value (best performance). The performance ranking positions of the considered correlations and models decreased in the order of modified Beggs & Brill (1973) correlation, modified Hagedorn & Brown (1965) correlation, Petalas & Aziz (2000) model, Poettmann & Carpenter (1952) correlation, Ansari et al. (1994) model and Hasan & Kabir (1988a) model. Notice that the performance positions of the correlations and models concerning E_3 changed as compared to the scenarios in which E_1 and E_2 were considered. Notice also that the performance ranking position of modified Beggs & Brill (1973) correlation was in third, second, and first positions when E_1, E_2, and E_3 were considered respectively.

The average error, E_4, represents the overall performance trend independent of the measured pressure drop [4-6]. The more negative is the value of E_4, the lower is the overall performance of the correlation or model and vice versa. As shown in Table 2, the most negative value of E_4 (-501.30 psia) was achieved by the Ansari et al. (1994) model, implying the worst overall performance. On the other hand, the Hagedorn & Brown (1965) correlation achieved the least negative value of E_4 (-21.43 psia), implying best overall performance. The performance positions based on E_4 are the same as those based on E_1.

The absolute average error, E_5, represents the magnitude of the difference between the predicted and measured pressure drops independently of the measured pressure drop [4]. A low value of E_5 denotes good performance, whereas a high value denotes poor performance. As shown in Table 2, the highest value of E_5 (511.99 psia) was achieved by the Ansari et al. (1994) model, implying the worst performance. On the other hand, the modified Hagedorn & Brown (1965) correlation had the lowest value of E_5 (171.01 psia), indicating the best performance. Performance ranking positions based on E_5 are the same as those based on E_2.

Standard deviation, E_6, indicates the degree of error dispersal independent of the measured pressure drop [4]. A low value of E_6 indicates the least scattering of the results (best performance) while a high value indicates the most scattering of results (worst performance). As shown in Table 2 the Hasan & Kabir (1988a) model achieved the highest value of E_6 (5359.15 psia) implying the worst performance prediction. The modified Beggs & Brill (1973) correlation achieved the lowest value of E_6 (1760.84 psia), implying the best performance prediction. Performance ranking positions based on E_6 are same as those based on E_3.

Relative performance factor, F_{rp} was recommended by Ansari et al. (1994) for making a comparison between correlations and models with a minimum value of 0 for the best performance prediction and a maximum value of 6 for the worst performance prediction. As shown in Table 2 Ansari et al. (1994) model achieved the maximum value of F_{rp} (5.84), implying the worst performance prediction. The modified Hagedorn & Brown (1965) correlation achieved the minimum value of F_{rp} (0.38), implying the best performance prediction. Performance ranking positions based on F_{rp} are the same as those based on E_2 and E_5.

Overall, the modified Hagedorn & Brown (1965) correlation gave the best performance prediction results for E_1, E_2, E_4, E_5, and F_{rp} whereas the modified Beggs & Brill (1973) correlation achieved the best results for E_3 and E_6. Equally, the Ansari et al. (1994) model achieved the worst performance prediction results for E_1, E_2, E_4, E_5, and F_{rp} while the Hasan & Kabir (1988a) model achieved the worst results for E_3 and E_6.

Relative performance factor, F_{rp} is the most important statistical error parameter because it incorporates the effects of the statistical errors and deviations (E_1, E_2, E_3, E_4, E_5 and E_6) as defined in Equation (22). Hence the modified Hagedorn & Brown (1965) correlation performed best with F_{rp} of 0.38 while the Ansari et al. (1994) model performed worst with F_{rp} of 5.84. The modified Beggs & Brill (1973) correlation, Poettmann & Carpenter (1952) correlation, Petalas & Aziz (2000) model, and Hasan & Kabir (1988a) model are in positions 2, 3, 4, and 5 respectively. The results clearly show that the empirical correlations outperformed the mechanistic models.

5.2. Discussion on Graphical Error Analysis

5.2.1. Discussion on Cross-plots

Figure 1 shows measured and predicted pressure drops cross-plots for Poettmann & Carpenter (1952) correlation, modified Hagedorn & Brown (1965) correlation, modified Beggs & Brill (1973) correlation, Ansari et al. (1994) model, Hasan & Kabir (1988a) model, and Petalas & Aziz (2000) model respectively. The closer the plotted points are to the unit slope line, the better is the correlation between the predicted and measured pressure drop (Ayoub, 2004). The best performing correlation or model should have the most number of plotted points falling within the $\pm 20\%$ deviation lines while the worst performing correlation should have the least number of plotted points falling within the $\pm 20\%$ deviation lines. A close examination of Figure 1, showed that the modified Hagedorn & Brown (1965) correlation performed best because 92% of the plotted points fell within the $\pm 20\%$ deviation lines. The Ansari et al. (1994) model performed worst because only 50% of the plotted points fell within the $\pm 20\%$ deviation lines. Modified Beggs & Brill (1973) correlation, Poettmann & Carpenter (1952) correlation, Petalas & Aziz (2000) model and Hasan & Kabir (1988a) model have 90%, 75%, 70%, and 60% respectively of the plotted points falling within the $\pm 20\%$ deviation lines and hence are on second, third, fourth and fifth performance positions respectively. The modified Hagedorn & Brown (1965) correlation and modified Beggs & Brill (1973) correlation showed a good correlation with the measured pressure drop while the other correlations and models tend to underestimate the pressure drop.

5.2.2. Discussion on Residual Plots

Figure 2 shows residual plots for the Poettmann & Carpenter (1952) correlation, modified Hagedorn & Brown (1965) correlation, modified Beggs & Brill (1973) correlation, Ansari et al. (1994) model, Hasan & Kabir (1988a) model, and Petalas & Aziz (2000) model respectively. The best-performing correlation or model should have the most number of plotted points falling within the $\pm 300\ psia$ residual deviation lines while the worst-performing correlation should have the least number of plotted points falling within the $\pm 300\ psia$ residual deviation lines. A close investigation of Figure 2 shows that prediction performance ranking from best to worst is modified Hagedorn & Brown (1965) correlation, modified Beggs & Brill (1973) correlation, Poettmann & Carpenter (1952) correlation, Petalas & Aziz (2000) model, Hasan & Kabir (1988a) model, and Ansari et al. (1994) model.

5.3. Discussion on Trend Analysis Results

Figure 3 shows plots of the relative error versus the percent of tubing with slug flow predicted by Ansari et al. (1994) model, churn flow by Hasan & Kabir (1988a) model, and slug flow by Petalas & Aziz (2000) model. Figure 3 clearly shows a downward trend for all investigated mechanistic models which is an indication of under-prediction of the pressure drop as the percentage of tubing with a slug or churn flow predicted by the respective investigated mechanistic models. This is a clear indication that the Ansari et al. (1994) slug flow, Hasan & Kabir (1988a) churn flow and Petalas & Aziz (2000) slug flow models under-predict the pressure drop. The gentle slope of the Petalas & Aziz (2000) trend line suggests moderate under-prediction by the Petalas & Aziz (2000) slug flow model while the steep slope of the Hasan & Kabir (1988a) implies severe under-prediction by the Hasan & Kabir (1988a) churn flow model.

6. Conclusions and Recommendations

6.1. Conclusions

Comparative performance analysis of models for predicting multiphase flow behavior in wellbores is presented and the following can be concluded from the oil field well datasets analyzed in this study.

i. The modified Hagedorn & Brown (1965) and modified Beggs & Brill (1973) correlations showed the best estimation of the pressure drop. This good prediction by both category C correlations is because of the large-scale data employed in developing the correlations and the modifications made to the correlations.

ii. The Ansari et al. (1994) and Hasan & Kabir (1988a) models showed severe underprediction of the pressure drop because the mechanistic models underpredicted the pressure drop whenever slug flow is predicted for the Ansari et al. (1994) model and churn flow for the Hasan & Kabir (1988a) model.

iii. Petalas & Aziz's (2000) model showed moderate underprediction of the pressure drop because the mechanistic model moderately underpredicted the pressure drop when slug flow is predicted.

iv. A solution procedure is proposed that eliminates the issue of non-convergent solutions.

6.2. Recommendations

The modified Hagedorn & Brown (1965) and modified Beggs & Brill (1973) correlations performed best because of the modifications made to the correlations. More study is needed to modify and improve the Ansari et al. (1994) and Petalas & Aziz (2000) slug flow models and Hasan & Kabir (1988a) churn flow model.

Nomenclature

Δp	Pressure drop, psia
p	Pressure, psia
$\bar{\rho}_{mn}$	Average no-slip mixture density, lb/ft^3
f_{2F}	Two-phase friction factor
v_m	Mixture velocity, ft/sec
v_{sg}	Gas superficial velocity, ft/sec
Δh	Length of tubing segment, ft
d	Diameter of tubing segment, $inch$
ρ_{ms}	Slip mixture density, lb/ft^3
ρ_{mn}	Slip mixture density, lb/ft^3
f_n	Normalizing friction factor
λ_L	No-slip liquid holdup
N_{Fr}	Froude number
E_k	Dimensionless kinetic energy
$\left(\frac{dp}{dL}\right)_{el}$	Elevation component of pressure gradient, psi/ft
$\left(\frac{dp}{dL}\right)_f$	Friction component of pressure gradient, psi/ft
$\left(\frac{dp}{dL}\right)_t$	Total pressure gradient, psi/ft
q_{gsc}	Gas production rate, $Mscf/day$
q_{osc}	Oil production rate, stb/day
q_{wsc}	Water production rate, stb/day
$R_{so}(k)$	Solution gas-oil ratio of kth tubing segment, scf/stb
$R_{sw}(k)$	Solution gas-water ratio of kth tubing segment, scf/stb
$B_g(k)$	Gas formation volume factor of kth tubing segment, ft^3/scf
$B_o(k)$	Oil formation volume factor of kth tubing segment, rb/stb
$B_w(k)$	Water formation volume factor of kth tubing segment, rb/stb
$q_g(k)$	Gas in-situ volumetric flow rate of kth tubing segment, ft^3/sec
$q_o(k)$	Oil in-situ volumetric flow rate of kth tubing segment, ft^3/sec
$q_w(k)$	Water in-situ volumetric flow rate of kth tubing segment, ft^3/sec
$\Delta p_{i_{meas}}$	Measured pressure drop, psia
$\Delta p_{i_{pred}}$	Predicted pressure drop, psia
$p_{bhi_{meas}}$	Measured bottom-hole pressure, psia
$p_{bhi_{pred}}$	Predicted bottom-hole pressure, psia
$p_{whi_{meas}}$	Measured wellhead pressure, psia
e_{ri}	Relative error of the ith data set
e_i	Actual error of the ith data set
E_1	Average percent error, %
E_2	Absolute average percent error, %
E_3	Percent standard deviation, %
E_4	Average error, psi
E_5	Absolute average error, psia
E_6	Standard deviation, psia
F_{rp}	Relative performance factor
N_{TS}	Number of tubing segments
N_{FL}	Number of tubing segments with slug flow or churn flow predicted
P_{FL}	Percent of tubing with slug flow or churn flow predicted
NCS	Non-Convergent Solutions
ML	Machine Learning
ANN	Artificial Neural Network
PC	Poettmann & Carpenter (1952) correlation
HB	Hagedorn & Brown (1965) correlation
BB	Beggs & Brill (1973) correlation with Payne et al. (1979) correction
AN	Ansari et al. (1994) model
HK	Hasan & Kabir (1988a) model
PA	Petalas & Aziz (2000) model

References

[1] Almutairi Z., Al-Alweet F. M., Alghamdi Y. A., Almisned O. A., Alothman O. Y.: Investigating the Characteristics of Two-Phase Flow Using Electrical Capacitance Tomography (ECT) for Three Pipe Orientations. Processes, **8**, (2020). DOI: 10.3390/pr8010051

[2] Brennen C. E., Brennen C. E.: Fundamentals of multiphase flow. (2005).
[3] Wallis G. B.: One-dimensional two-phase flow, Courier Dover Publications (2020).
[4] Ansari A. M., Sylvester N. D., Sarica C., Shoham O., Brill J. P.: A Comprehensive Mechanistic Model for Upward Two-Phase Flow in Wellbores. SPE Production & Facilities, **9**, 143-151 (1994). DOI: 10.2118/20630-PA
[5] Kaya A. S., Sarica C., Brill J. P.: Comprehensive Mechanistic Modeling of Two-Phase Flow in Deviated Wells. in SPE Annual Technical Conference and Exhibition. (1999 of Conference). DOI: 10.2118/56522-MS
[6] Kaya A. S., Sarica C., Brill J. P.: Mechanistic Modeling of Two-Phase Flow in Deviated Wells. SPE Production & Facilities, **16**, 156-165 (2001). DOI: 10.2118/72998-PA
[7] Zhang H.-Q., Wang Q., Sarica C., Brill J. P.: Unified Model for Gas-Liquid Pipe Flow via Slug Dynamics—Part 1: Model Development. Journal of Energy Resources Technology, **125**, 266-273 (2003). DOI: 10.1115/1.1615246
[8] Zhang H.-Q., Sarica C.: Unified Modeling of Gas/Oil/Water Pipe Flow - Basic Approaches and Preliminary Validation. in SPE Annual Technical Conference and Exhibition. (2005 of Conference). DOI: 10.2118/95749-MS
[9] Yahaya A. U., Al Gahtani A.: A Comparative Study Between Empirical Correlations & Mechanistic Models of Vertical Multiphase Flow. in SPE/DGS Saudi Arabia Section Technical Symposium and Exhibition. (2010 of Conference). DOI: 10.2118/136931-MS
[10] Kokal S. L.: An Experimental study of two phase flow in inclined pipes, (1987).
[11] Brill J. P., Arirachakaran S. J.: State of the Art in Multiphase Flow. Journal of Petroleum Technology, **44**, 538-541 (1992). DOI: 10.2118/23835-PA
[12] Dukler A. E., Hubbard M. G.: A model for gas-liquid slug flow in horizontal and near horizontal tubes. Industrial & Engineering Chemistry Fundamentals, **14**, 337-347 (1975).
[13] Luo C., Zhang L., Liu Y., Zhao Y., Xie C., Wang L., Wu P.: An improved model to predict liquid holdup in vertical gas wells. Journal of Petroleum Science and Engineering, **184**, 106491 (2020). DOI: https://doi.org/10.1016/j.petrol.2019.106491
[14] Wu B., Firouzi M., Mitchell T., Rufford T. E., Leonardi C., Towler B.: A critical review of flow maps for gas-liquid flows in vertical pipes and annuli. Chemical Engineering Journal, **326**, 350-377 (2017). DOI: https://doi.org/10.1016/j.cej.2017.05.135
[15] Barnea D., Shoham O., Taitel Y., Dukler A. E.: Flow pattern transition for gas-liquid flow in horizontal and inclined pipes. Comparison of experimental data with theory. International journal of multiphase flow, **6**, 217-225 (1980).
[16] Abduvayt P., Manabe R., Arihara N.: Effects of Pressure and Pipe Diameter on Gas-Liquid Two-Phase Flow Behavior in Pipelines. in SPE Annual Technical Conference and Exhibition. (2003 of Conference). DOI: 10.2118/84229-MS
[17] Farokhpoor R., Liu L., Langsholt M., Hald K., Amundsen J., Lawrence C.: Dimensional analysis and scaling in two-phase gas–liquid stratified pipe flow–Methodology evaluation. International Journal of Multiphase Flow, **122**, 103139 (2020). DOI: https://doi.org/10.1016/j.ijmultiphaseflow.2019.103139
[18] Brill J. P., Mukherjee H.: Multiphase flow in wells. Society of Petroleum Engineers of AIME, (1999).
[19] Ayoub M. A.: Development and testing of an artificial neural network model for predicting bottomhole pressure in vertical multiphase flow. (2005).
[20] Baxendell P. B., Thomas R.: The Calculation of Pressure Gradients In High-Rate Flowing Wells. Journal of Petroleum Technology, **13**, 1023-1028 (1961). DOI: 10.2118/2-PA
[21] Fancher G. H., Jr., Brown K. E.: Prediction Of Pressure Gradients For Multiphase Flow In Tubing. in Fall Meeting of the Society of Petroleum Engineers of AIME. (1962 of Conference). DOI: 10.2118/440-MS
[22] Poettman F. H., Carpenter P. G.: The multiphase flow of gas, oil, and water through vertical flow strings with application to the design of gas-lift installations. OnePetro (1952).
[23] Asheim H.: MONA, An Accurate Two-Phase Well Flow Model Based on Phase Slippage. SPE Production Engineering, **1**, 221-230 (1986). DOI: 10.2118/12989-PA
[24] Hagedorn A. R., Brown K. E.: Experimental Study of Pressure Gradients Occurring During Continuous Two-Phase Flow in Small-Diameter Vertical Conduits. Journal of Petroleum Technology, **17**, 475-484 (1965). DOI: 10.2118/940-PA
[25] Beggs D. H., Brill J. P.: A Study of Two-Phase Flow in Inclined Pipes. Journal of Petroleum Technology, **25**, 607-617 (1973). DOI: 10.2118/4007-PA
[26] Duns H., Jr., Ros N. C. J.: Vertical flow of gas and liquid mixtures in wells. in 6th World Petroleum Congress. (1963 of Conference).
[27] Orkiszewski J.: Predicting Two-Phase Pressure Drops in Vertical Pipe. Journal of Petroleum Technology, **19**, 829-838 (1967). DOI: 10.2118/1546-PA
[28] Gomez L. E., Shoham O., Schmidt Z., Chokshi R. N., Northug T.: Unified Mechanistic Model for Steady-State Two-Phase Flow: Horizontal to Vertical Upward Flow. SPE Journal, **5**, 339-350 (2000). DOI: 10.2118/65705-PA

[29] Jahanandish I., Salimifard B., Jalalifar H.: Predicting bottomhole pressure in vertical multiphase flowing wells using artificial neural networks. Journal of Petroleum Science and Engineering, **75**, 336-342 (2011). DOI: https://doi.org/10.1016/j.petrol.2010.11.019

[30] Kanin E. A., Osiptsov A. A., Vainshtein A. L., Burnaev E. V.: A predictive model for steady-state multiphase pipe flow: Machine learning on lab data. Journal of Petroleum Science and Engineering, **180**, 727-746 (2019). DOI: https://doi.org/10.1016/j.petrol.2019.05.055

[31] Li X., Miskimins J. L., Hoffman B. T.: A Combined Bottom-hole Pressure Calculation Procedure Using Multiphase Correlations and Artificial Neural Network Models. in SPE Annual Technical Conference and Exhibition. (2014 of Conference). DOI: 10.2118/170683-MS

[32] Sami N. A., Ibrahim D. S.: Forecasting multiphase flowing bottom-hole pressure of vertical oil wells using three machine learning techniques. Petroleum Research, **6**, 417-422 (2021). DOI: https://doi.org/10.1016/j.ptlrs.2021.05.004

[33] Brill J. P.: Multiphase Flow in Wells. Journal of Petroleum Technology, **39**, 15-21 (1987). DOI: 10.2118/16242-PA

[34] Guo B., Ghalambor A.: Gas volume requirements for underbalanced drilling: deviated holes, PennWell Corporation (2002).

[35] Ros N. C. J.: Simultaneous Flow of Gas and Liquid As Encountered in Well Tubing. Journal of Petroleum Technology, **13**, 1037-1049 (1961). DOI: 10.2118/18-PA

[36] Beggs H. D.: Production Optimization Using Nodal (TM) Analysis, OGCI (2003).

[37] Griffith P., Wallis G. B.: Two-phase slug flow. Journal of Heat Transfer, **83**, (1961).

[38] Mukherjee H., Brill J. P.: Pressure Drop Correlations for Inclined Two-Phase Flow. Journal of Energy Resources Technology, **107**, 549-554 (1985). DOI: 10.1115/1.3231233

[39] Brill J. P., Beggs H. D.: Two-Phase Flow in Pipes, ed. t. Edition, Tulsa University Press (1991).

[40] Payne G. A., Palmer C. M., Brill J. P., Beggs H. D.: Evaluation of Inclined-Pipe, Two-Phase Liquid Holdup and Pressure-Loss Correlation Using Experimental Data (includes associated paper 8782). Journal of Petroleum Technology, **31**, 1198-1208 (1979). DOI: 10.2118/6874-PA

[41] Ouyang L.-B., Aziz K.: A MECHANISTIC MODEL FOR GAS–LIQUID FLOW IN HORIZONTAL WELLS WITH RADIAL INFLUX OR OUTFLUX. Petroleum Science and Technology, **20**, 191-222 (2002). DOI: 10.1081/LFT-120002095

[42] Xiao J. J., Shonham O., Brill J. P.: A Comprehensive Mechanistic Model for Two-Phase Flow in Pipelines. in SPE Annual Technical Conference and Exhibition. (1990 of Conference). DOI: 10.2118/20631-MS

[43] Taitel Y., Dukler A. E.: A model for predicting flow regime transitions in horizontal and near horizontal gas-liquid flow. AIChE Journal, **22**, 47-55 (1976). DOI: https://doi.org/10.1002/aic.690220105

[44] Hasan A. R., Kabir C. S.: A Study of Multiphase Flow Behavior in Vertical Wells. SPE Production Engineering, **3**, 263-272 (1988). DOI: 10.2118/15138-PA

[45] Ozon P. M., Ferschneider G., Chwetzoff A.: A New Multiphase Flow Model Predicts Pressure And Temperature Profiles In Wells. in SPE Offshore Europe. (1987 of Conference). DOI: 10.2118/16535-MS

[46] Hasan A. R., Kabir C. S.: Predicting Multiphase Flow Behavior in a Deviated Well. SPE Production Engineering, **3**, 474-482 (1988). DOI: 10.2118/15449-PA

[47] Taitel Y., Barnea D., Dukler A. E.: Modelling flow pattern transitions for steady upward gas-liquid flow in vertical tubes. AIChE Journal, **26**, 345-354 (1980). DOI: https://doi.org/10.1002/aic.690260304

[48] Petalas N., Aziz K.: A Mechanistic Model for Multiphase Flow in Pipes. Journal of Canadian Petroleum Technology, **39**, (2000). DOI: 10.2118/00-06-04

[49] Abdul-Majeed G. H., Kadhim F. S., Almahdawi F. H. M., Al-Dunainawi Y., Arabi A., Al-Azzawi W. K.: Application of artificial neural network to predict slug liquid holdup. International Journal of Multiphase Flow, **150**, 104004 (2022). DOI: https://doi.org/10.1016/j.ijmultiphaseflow.2022.104004

[50] Abdul-Majeed G. H., Al-Mashat A. M.: A mechanistic model for vertical and inclined two-phase slug flow. Journal of Petroleum Science and Engineering, **27**, 59-67 (2000). DOI: https://doi.org/10.1016/S0920-4105(00)00047-4

[51] Nwanwe C. C., Duru U. I., Nwanwe O. I., Chikwe A. O., Ojiabo K. T., Umeojiakor C. T.: Optimum tubing size prediction model for vertical multiphase flow during flow production period of oil wells. Journal of Petroleum Exploration and Production Technology, **10**, 2989-3005 (2020). DOI: 10.1007/s13202-020-00964-8

[52] Ahmed T.: Hydrocarbon phase behavior (1989).

[53] Standing M. B.: Volumetric and phase behavior of oil field hydrocarbon systems, Society of petroleum engineers of AIME, Dallas (1981).

[54] Gould T. L.: Vertical Two-Phase Steam-Water Flow in Geothermal Wells. Journal of Petroleum Technology, **26**, 833-842 (1974). DOI: 10.2118/4961-PA

[55] Márquez-Torres L., Ochoa-Pineda J., Pico P., Valdés J. P., Becerra D., Pinilla A., Pereyra E., Ratkovich N.: Comparison of 63 different void fraction correlations for different flow patterns, pipe inclinations, and liquid viscosities. SN Applied Sciences, **2**, 1695 (2020). DOI: 10.1007/s42452-020-03464-w

[56] Hao M., Lin Y., Zhao X.: A relative error-based approach for variable selection. Computational Statistics & Data Analysis, **103**, 250-262 (2016). DOI: https://doi.org/10.1016/j.csda.2016.05.013
[57] Shoham O.: Mechanistic modeling of gas-liquid two-phase flow in pipes. (2006).
[58] Ahmed M. M., Ayoub M. A.: A comprehensive study on the current pressure drop calculation in multiphase vertical wells; current trends and future prospective. (2013).